CRYSTALLOGRAPHIC
COMMUNICATIONS

ISSN: 2056-9890
journals.iucr.org/e

Crystal structures and Hirshfeld surface analyses of (*E*)-*N*′-benzylidene-2-oxo-2*H*-chromene-3-carbohydrazide and the disordered hemi-DMSO solvate of (*E*)-2-oxo-*N*′-(3,4,5-trimethoxybenzylidene)-2*H*-chromene-3-carbohydrazide: lattice energy and intermolecular interaction energy calculations for the latter

Ligia R. Gomes, John Nicolson Low, James L. Wardell, Camiola Capelini, Vitoria R.F. Câmara, Edson F. da Silva and Samir A. Carvalho

Acta Cryst. (2019). E**75**, 1403–1410

CRYSTALLOGRAPHIC
COMMUNICATIONS

ISSN 2056-9890

Received 20 August 2019
Accepted 29 August 2019

Edited by A. J. Lough, University of Toronto, Canada

Keywords: crystal structure; tuberculosis; Hirshfeld surface analysis; nitrogen-containing 2-oxo-2*H*-chromene derivative.

CCDC references: 1917252; 1917524

Supporting information: this article has supporting information at journals.iucr.org/e

Crystal structures and Hirshfeld surface analyses of (*E*)-*N*′-benzylidene-2-oxo-2*H*-chromene-3-carbohydrazide and the disordered hemi-DMSO solvate of (*E*)-2-oxo-*N*′-(3,4,5-trimethoxybenzylidene)-2*H*-chromene-3-carbohydrazide: lattice energy and intermolecular interaction energy calculations for the latter

Ligia R. Gomes,[a,b] John Nicolson Low,[c]* James L. Wardell,[c] Camiola Capelini,[d] Vitoria R.F. Câmara,[e,d] Edson F. da Silva[d] and Samir A. Carvalho[d]

[a]REQUIMTE, Departamento de Química e Bioquímica, Faculdade de Ciências da Universidade do Porto, Rua do Campo Alegre, 687, P-4169-007, Porto, Portugal, [b]FP-ENAS-Faculdade de Ciências de Saúde, Escola Superior de Saúde da UFP, Universidade Fernando Pessoa, Rua Carlos da Maia, 296, P-4200-150 Porto, Portugal, [c]Department of Chemistry, University of Aberdeen, Meston Walk, Old Aberdeen, AB24 3UE, Scotland, [d]Instituto de Tecnologia em Fármacos - Farmanguinhos, Fundaçâo Oswaldo Cruz, 21041-250 Rio de Janeiro, RJ, Brazil, and [e]Escola de Ciência e Tecnologia - ECT, Universidade do, Grande Rio - Unigranrio, 25071-202, Duque de Caxias, RJ, Brazil. *Correspondence e-mail: jnlow111@gmail.com

The crystal structures of the disordered hemi-DMSO solvate of (*E*)-2-oxo-*N*′-(3,4,5-trimethoxybenzylidene)-2*H*-chromene-3-carbohydrazide, $C_{20}H_{18}N_2O_6\cdot 0.5C_2H_6OS$, and (*E*)-*N*′-benzylidene-2-oxo-2*H*-chromene-3-carbohydrazide, $C_{17}H_{12}N_2O_3$ (**4**: $R = C_6H_5$), are discussed. The non-hydrogen atoms in compound [**4**: $R = (3,4,5\text{-MeO})_3C_6H_2$)] exhibit a distinct curvature, while those in compound, (**4**: $R = C_6H_5$), are essential coplanar. In (**4**: $R = C_6H_5$), C—H$\cdots$O and π–π intramolecular interactions combine to form a three-dimensional array. A three-dimensional array is also found for the hemi-DMSO solvate of [**4**: $R = (3,4,5\text{-MeO})_3C_6H_2$], in which the molecules of coumarin are linked by C—H$\cdots$O and C—H$\cdots\pi$ interactions, and form tubes into which the DMSO molecules are cocooned. Hirshfeld surface analyses of both compounds are reported, as are the lattice energy and intermolecular interaction energy calculations of compound (**4**: $R = C_6H_5$).

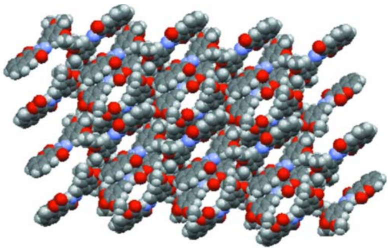

1. Chemical context

Tuberculosis (TB) is one of the world's most infectious killer diseases, claiming 4,500 lives each day (https://www.who.int/en/news-room/fact-sheets/detail/tuberculosis). The development of drug resistance to the first-line drugs seriously compounds the dangers of the disease. The latest multidrug-resistant TB data analysis shows that 4.1% of new and 19% of previously treated TB cases in the world are estimated to have rifampicin- or multidrug-resistant tuberculosis (MDR/RR-TB) and about 6.2% of the MDR-TB cases have additional drug resistance, extensively drug-resistant TB (XDR-TB) (www.who.int/tb/challenges/mdr/MDR-RR_TB_factsheet_2017.pdf). As a result of the increase of MDR-TB/XDR-TB and AIDS cases worldwide, associated with the lack of efficacy of available drugs, the discovery of new potent and safer drug-candidate prototypes able to treat this disease has become an urgent challenge.

https://doi.org/10.1107/S2056989019012015

Table 1
Selected bond lengths (Å) in the linker chain between the coumarin and phenyl moieties.

Bond	[**4**: *R* = 3,4,5-MeO$_3$C$_6$H$_2$·0.5DMSO]	(**4**: *R* = C$_6$H$_5$)
C2—O2	1.2133 (12)	1.2103 (11)
C31—O31	1.2234 (13)	1.2237 (12)
C3—C31	1.5056 (13)	1.5003 (13)
C31—N32	1.3543 (13)	1.3530 (13)
N32—N33	1.3793 (11)	1.3768 (11)
N33—C34	1.2753 (14)	1.2753 (13)
C34—C341	1.4629 (14)	1.4649 (13)

The *N*-acylhydrazone functional group, –C(O)—NH—N═CH–, is found in many compounds having important and diverse biological activities (Fraga & Barreiro, 2006; Singh *et al.*, 2016), including their use in the fight against tuberculosis, especially the drug-resistant forms (Cardoso *et al.*, 2011; Souza *et al.*, 2017). Specifically, *N*-acylhydrazonyl-containing 2*H*-chromene derivatives have been found to possess significant anti-mycobacterial activities (Angelova *et al.*, 2017; Cardoso *et al.*, 2011). The Angelova *et al.* (2017) study revealed compounds of type **1**–**3** (*R* = aryl) in the schematic diagram as having *in vitro* antimycobacterial activities against *Mycobacterium tuberculosis H37Rv* comparable to the first-line drugs, isoniazid (INH) and ethambutol, while the Cardoso *et al.* (2011) study indicated compounds of type **4** (*R* = aryl) in the schematic diagram to be active against *Mycobacterium* tuberculosis ATCC 27294. Of interest, **4** (*R* = 3-MeOC$_6$H$_4$) and (*R* = 4-MeOC$_6$H$_4$), but not **4** [*R* = 3,4-(MeO)$_2$C$_6$H$_3$] exhibited better activities than did pyrazinamide (Cardoso *et al.*, 2011).

We have continued studies of the *Mycobacterial* activities of compounds of type **4** (Capelini *et al.*, 2019) against various strains, namely *M. tuberculosis* H37Rv ATCC 27294 INH-resistant *Mtb*, multidrug-resistant *Mtb* and wild INH/RIF-resistant *Mtb* isolates: [**4**: *R* = (3,4,5-MeO)$_3$C$_6$H$_2$] exhibited significant activity against the INH resistant/RIP resistant strain, *M. tuberculosis* SR 5110/1116. We now wish to report the crystal structures and the Hirshfeld surface analyses of a DMSO hemi-solvate of this compound and also that of the parent compound, (**4**: *R* = C$_6$H$_5$), an inactive compound. In addition, lattice energy and intermolecular interaction energy calculations are reported for **4** (*R* = C$_6$H$_5$). This article also continues our reporting of the structures of nitrogen-containing 2-oxo-2*H*-chromene derivatives (Gomes *et al.*, 2016*a*).

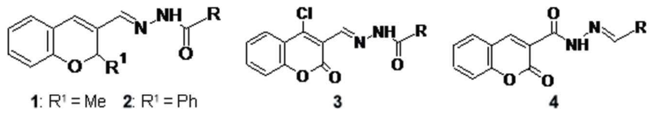

1: R^1 = Me **2**: R^1 = Ph **3** **4**

2. Structural commentary

The solvate [**4**: *R* = (3,4,5-MeO)$_3$C$_6$H$_2$·0.5DMSO] crystallizes in the orthorhombic space group *C*2/*c*, with one molecule of the coumarin and with a half DMSO solvate molecule spread over two symmetry-related sites in the asymmetric unit, Fig. 1. Compound (**4**: *R* = C$_6$H$_5$) crystallizes in the triclinic space group $P\overline{1}$ with one molecule in the asymmetric unit, see Fig. 2. The geometry about the C═N bond of the hydrazine moiety is (*E*) in both cases. There are intramolecular C2—H2···O1 and C4—H4···O31 hydrogen bonds (Tables 2 and 3) present in both molecules. The non-hydrogen atoms, with the additional exclusion of atoms in the three methoxy groups in the phenyl substituent unit of [**4**: *R* = (3,4,5-MeO)$_3$C$_6$H$_2$·0.5DMSO], form a distinctively curved arrangement, as illustrated in Fig. 1*b*. In contrast, the non-hydrogen atoms in (**4**: *R* = C$_6$H$_5$) are essentially co-planar, see Fig. 3. The bond lengths in the linker chain between the coumarin and phenyl moieties are indicative of electronic delocalization, see Table 1.The interplanar angles, coumarin/linker, linker/phenyl and phenyl/coumarin in [**4**: *R* = (3,4,5-MeO)$_3$C$_6$H$_2$·0.5DMSO], are 7.70 (7), 11.43 (8) and 14.97 (5)°, compared to 2.89 (5), 5.07 (5) and 7.05 (4)°, respectively, in (**4**: *R* = C$_6$H$_5$). In [**4**: *R* = (3,4,5-MeO)$_3$C$_6$H$_2$], as expected for a compound with adjacent methoxy groups on the 3,4 and 5 positions of a phenyl ring, the middle methoxy group is out of the plane of its phenyl group (see, for example, Peralta *et al.*, 2007; Howie *et al.*, 2010; Gomes *et al.*, 2016*b*).

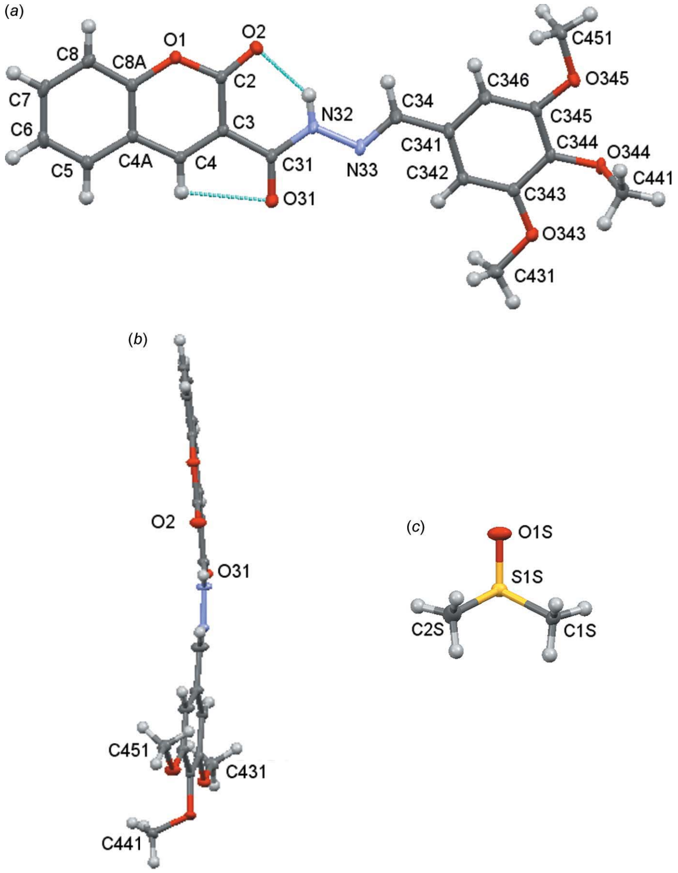

Figure 1
Compound [**4**: *R* = 3,4,5-(MeO)$_3$C$_6$H$_2$·0.5DMSO]. (*a*) Molecular structure and numbering scheme for [**4**: *R* = 3,4,5-(MeO)$_3$C$_6$H$_2$] with displacement ellipsoids drawn at the 50% level, (*b*) side-on view of the conformation of [**4**: *R* = 3,4,5-(MeO)$_3$C$_6$H$_2$] and (*c*) the DMSO hemi-solvate showing one component of disorder.

Table 2
Hydrogen-bond geometry (Å, °) for [**4**: *R* = (3,4,5-MeO)$_3$C$_6$H$_2$·0.5DMSO].

*Cg*1, *Cg*2 and *Cg*3 are the centroids of the O1/C2–C4/C4*A*/C8*A*, C4*A*/C5–C8/C8*A* and C341–C346 rings, respectively.

D—H···A	D—H	H···A	D···A	D—H···A
N32—H32···O2	0.870 (16)	1.955 (15)	2.6878 (12)	141.0 (14)
C441—H41*C*···O345^{i}	0.98	2.58	3.4772 (12)	152
C451—H51*A*···O1^{ii}	0.98	2.65	3.4463 (13)	138
C34—H34···O1*S*	0.95	2.57	3.30 (5)	134
C34—H34···O1*S*^{ii}	0.95	2.63	3.34 (5)	133
C34—H34···S1*S*	0.95	2.69	3.6158 (12)	166
C431—H43*C*···O343^{iii}	0.98	2.50	3.2505 (13)	133
C2*S*—H2*SA*···N32^{iv}	0.98	2.61	3.3000 (6)	127
C4—H4···O31	0.95	2.45	2.7761 (12)	100
C4—H4···O31^{v}	0.95	2.38	3.2415 (12)	150
C5—H5···O31^{v}	0.95	2.59	3.3931 (13)	143
C431—H43*B*···*Cg*3^{vi}	0.98	2.73	3.5882 (13)	147
C451—H51*B*···*Cg*3^{vi}	0.98	2.95	3.8562 (12)	155
C451—H51*C*···*Cg*2^{vii}	0.98	2.83	3.6883 (13)	147
C31—O31···*Cg*1^{vii}	0	0	3.3971 (6)	90 (1)

Symmetry codes: (i) $-x+\frac{3}{2}, -y+\frac{3}{2}, -z+2$; (ii) $-x+1, y, -z+\frac{3}{2}$; (iii) $-x+\frac{3}{2}, y-\frac{1}{2}, -z+\frac{3}{2}$; (iv) $-x+1, y+1, -z+\frac{3}{2}$; (v) $-x+1, -y, -z+1$; (vi) $x, y-1, z$; (vii) $-x+1, -y+1, -z+1$.

3. Supramolecular features

3.1. Intermolecular interactions

There are no classical intermolecular O—H···*X* (*X* = O or N) in the crystal of [**4**: *R* = (3,4,5-MeO)$_3$C$_6$H$_2$·0.5DMSO]: the molecules of [**4**: *R* = (3,4,5-MeO)$_3$C$_6$H$_2$] are linked by a number of C—H···O and C—H···π hydrogen bonds (Table 3) and by a C═O···π(1) interaction: the three rings in compounds **4** have been given the designations π(1) for the O1/C2–C4/C4*A*/C8*A*, π(2) for the C4*A*/C5–C8/C8*A* and π(3) for the C341–C346 rings with centroids *Cg*1, *Cg*2 and *Cg*3, respectively. A two-molecule wide column is generated from a combination of the C4—H4···O31, C5—C5···O31 and C441—H41*C*···O345 hydrogen bonds, see Fig. 3*a*. Within the columns, the C4—H4···O31 and C5—H5···O31 interactions generate $R^1_2(5)$ rings and pairs of the C441—H41*C*···O345 hydrogen bonds lead to $R^2_2(12)$ rings. These two-molecule-wide columns are linked by the carbonyl–arene interaction

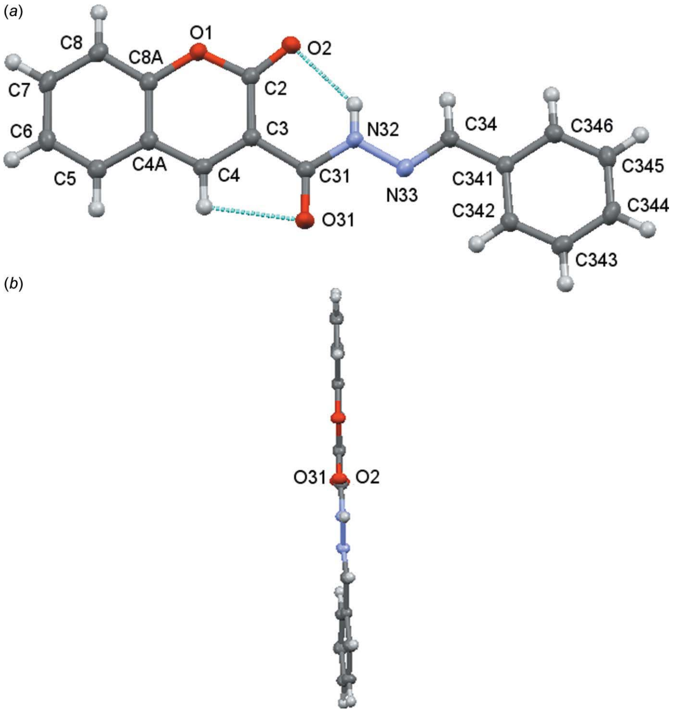

Figure 2
Compound (**4**: *R* = C$_6$H$_5$). (*a*) Molecular structure and numbering scheme with displacement ellipsoids drawn at the 50% level and (*b*) side-on view of the conformation.

Table 3
Hydrogen-bond geometry (Å, °) for (**4**: *R* = C$_6$H$_5$).

D—H···A	D—H	H···A	D···A	D—H···A
N32—H1···O2	0.857 (15)	2.062 (15)	2.7238 (10)	133.5 (12)
C34—H34···O2^{i}	0.95	2.54	3.4417 (11)	159
C4—H4···O31	0.95	2.40	2.7415 (11)	101
C4—H4···O31^{ii}	0.95	2.28	3.1377 (12)	149
C5—H5···O31^{ii}	0.95	2.57	3.3456 (12)	139
C346—H346···O1^{i}	0.95	2.63	3.5195 (11)	156

Symmetry codes: (i) $-x, -y+1, -z+1$; (ii) $-x+2, -y, -z+1$.

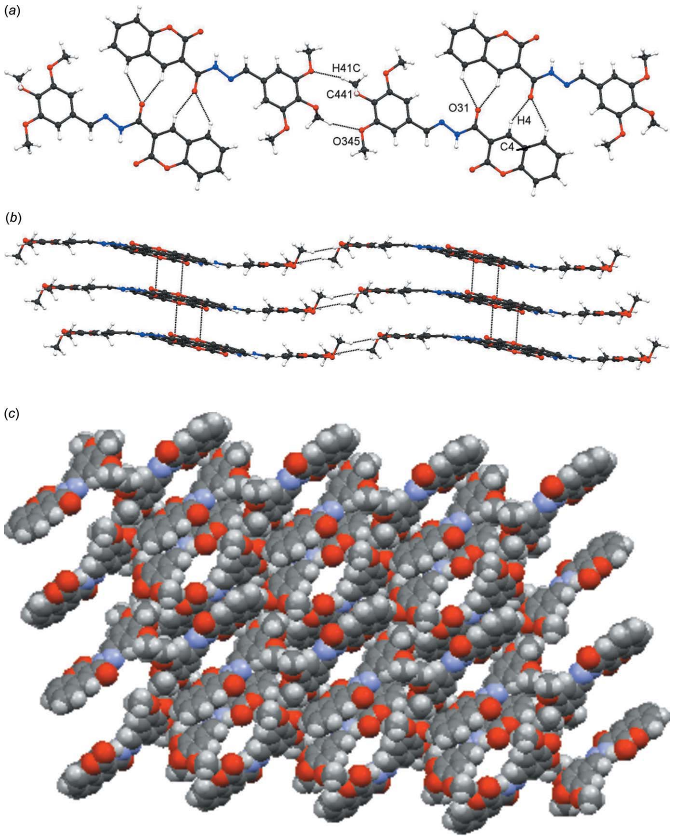

Figure 3
Compound [**4**: *R* = 3,4,5-(MeO)$_3$C$_6$H$_2$·0.5DMSO]. (*a*) A two-molecule-wide column of molecules, formed from C4—H4···O31, C5—H5···O31 and C441—H41*C*···O345 hydrogen bonds, (*b*) columns linked into undulating sheets by C31═O31···π(1) interactions and (*c*) a spiral of molecules, which creates a channel into which the disordered solvate molecules are held by a number of C—H···X (*X* = O, N or S) hydrogen bonds: the channel is generated from C431–H43*B*···π(3), C451—H51*B*···π(3) and C451—H51*C*···π(2) interactions and lies along the crystallographic twofold axis.

C31═O31···π(1) into undulating sheets, see Fig. 3*b*. A further structural subset is formed from a series of C—H···π interactions: C431—H43*B*···π(3) and C451—H51*B*···π(3) separately form chains of [**4**: *R* = (3,4,5-MeO)$_3$C$_6$H$_2$] propagating in the *b*-axis direction, while the C451—H51*C*···π2 interaction generates a spiral chain of molecules; together these three interactions form a tube, into which the disordered DMSO molecule is cocooned, held there by a number of C—H···*X* (*X* = O, N and S) hydrogen bonds. A view of the channels in which the the disordered DMSO sits is shown in Fig. 3*c*. These channels run along the crystallographic twofold axis.

The intermolecular interactions in compound (**4**: *R* = C$_6$H$_5$) are C—H···O hydrogen bonds, see Table 3, and π–π stacking interactions. Symmetric dimers are formed from pairs of each of C4—H4···O31 and C5—H5···O31, see Fig. 4*a*. Within the dimers are two $R_2^1(5)$ and one $R_2^2(10)$ rings. These dimers are then linked by pairs of C34—H34···O2 and C346—H346···O1 hydrogen bonds into a one-molecule-wide column, generating two $R_2^2(8)$ and one $R_2^2(16)$ rings. A second substructure is formed from alternating π–π$^{\rm i}$ and π–π$^{\rm ii}$ interactions, involving the C4*A*/C5–C8/C8*A* ring with centroid *Cg*2 and the C341–C346 ring with centroid *Cg*3, see Fig. 4*b* [symmetry codes: (i) 1 − *x*, −*y*, 1 − *z*; (ii) 1 − *x*, 1 − *y*, 1 − *z*]. The π–π$^{\rm i}$ interaction is considered to be the stronger, both from the *Cg*···*Cg* separation [3.8417 (6) compared to 4.1750 (6) Å] and from its greater π overlap, average slippages being 1.820 and 2.325 Å (the rings are inclined to each other). Further confirmation of the relative importance of the two interactions comes from the energy calculations, see Section 3.3. The combination of all the intermolecular interactions provides a three-dimensional arrangement.

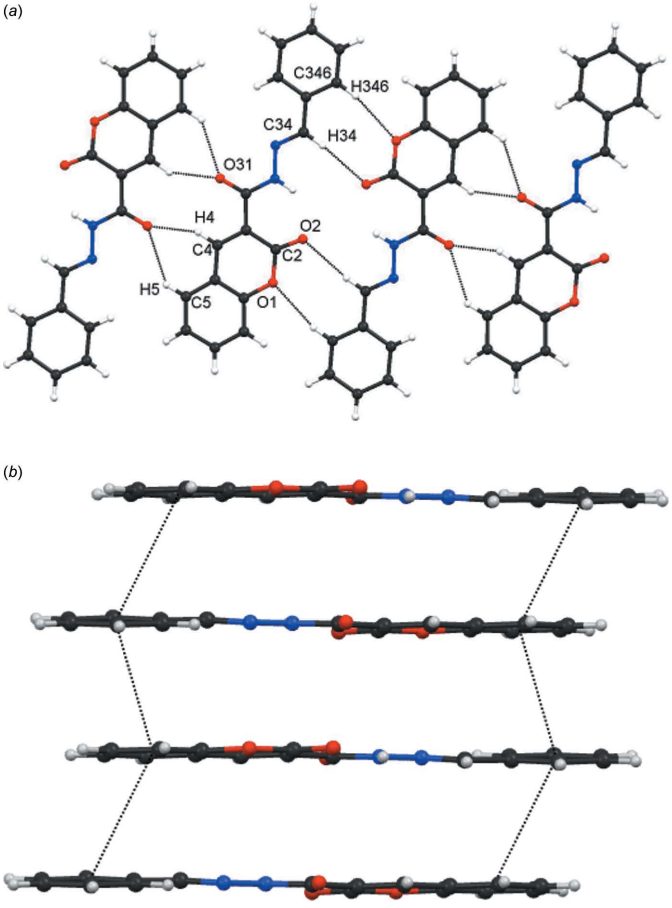

Figure 4
Compound (**4**: *R* = C$_6$H$_5$). (*a*) Part of a one-molecule-wide column formed from linking molecules by a combination of C4—H4···O31, and C5—H5···O31, C34—H34···O2 and C346—H346···O1 hydrogen bonds. Within these columns are $R_2^1(5)$, $R_2^2(10)$ and $R_2^2(16)$ rings and (*b*) part of a column formed from two alternating π–π$^{\rm i}$ and π–π$^{\rm ii}$ interactions [symmetry codes: (i) 1 − *x*, −*y*, 1 − *z*; (ii) 1 − *x*, 1 − *y*, 1 − *z*].

3.2. Hirshfeld Surface analyses

Hirshfeld surfaces (Spackman & Jayatilaka, 2009) and two-dimensional fingerprint (FP) plots (Spackman & McKinnon, 2002), provide complementary information concerning the intermolecular interactions discussed above. The analyses were generated using *CrystalExplorer3.1* (Wolff *et al.*, 2012). The Hirshfeld surfaces mapped over $d_{\rm norm}$ were scaled between −0.33 and 1.23, and are shown in Fig. 5 for [**4**: *R* = (3,4,5-MeO)$_3$C$_6$H$_2$·0.5DMSO] and in Fig. 6 for (**4**: *R* = C$_6$H$_5$). The red areas on the surfaces correspond to close contacts,

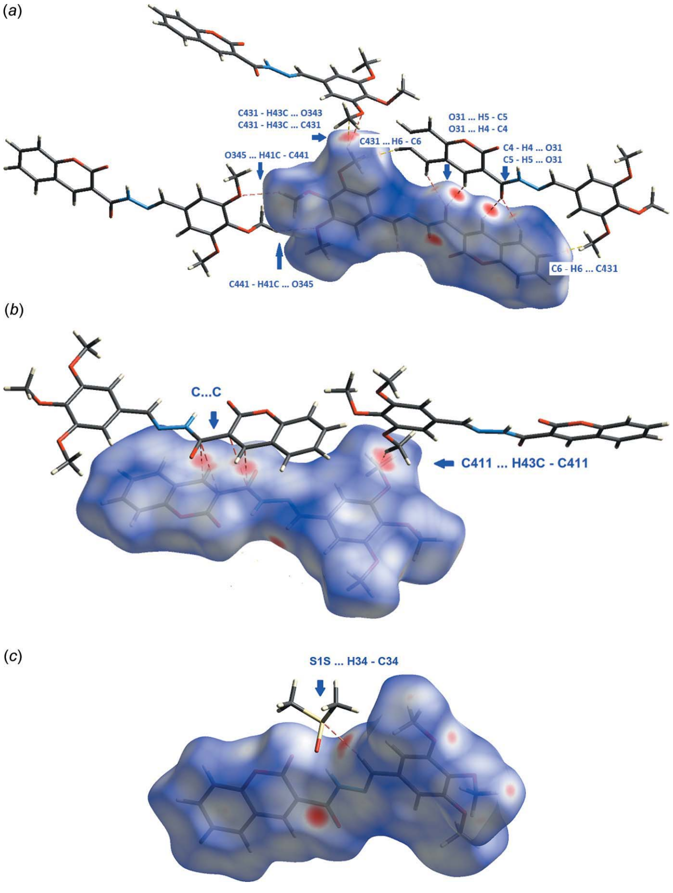

Figure 5
Hirshfeld surface views for [**4**: *R* = 3,4,5-(MeO)$_3$C$_6$H$_2$·0.5DMSO]. The red areas on the surfaces correspond to close contacts. In (*a*) the site of a close H6···C431 contract is indicated: H6···C431$^{\rm i}$ = 2.85 Å (sum of contact radii = 2.90 Å) [symmetry code: (i) 1 − *x*, −*y*, 1 − *z*].

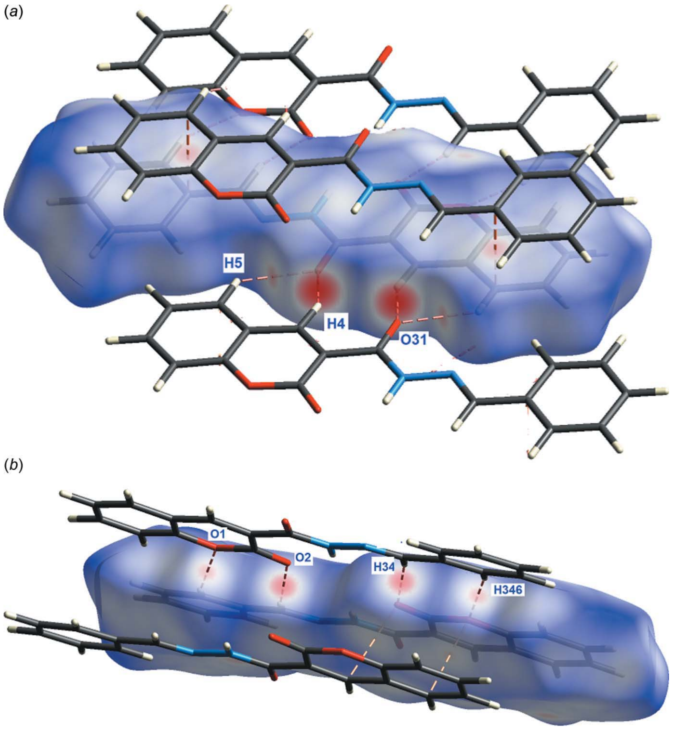

Figure 6
Two views of the Hirshfeld surface of (**4**: $R = C_6H_5$)·The red areas on the surfaces correspond to the designated close contacts.

and have been designated. The FP plots for [**4**: R = (3,4,5-MeO)$_3$C$_6$H$_2$·0.5(DMSO)] and (**4**: $R = C_6H_5$) are shown in Fig. 7*a* and 7*b*, respectively. The blue spikes in the FP plot for (**4**: $R = C_6H_5$) ending at (1.2; 0.9) and (0.9;1.1) relate to O···H/H···O contacts and the high intensity of pixels, green and red areas relate to C···C contacts.

The percentages of atom···atom close contacts are listed in Table 4. Leaving the H···H contacts aside, the highest percentages of atom···atom close contacts for [**4**: R = (3,4,5-MeO)$_3$C$_6$H$_2$·0.5DMSO], are 28.4 and 23.7% for H···O/O···H and H···C/C···H, respectively. The corresponding values for (**4**: $R = C_6H_5$) are 20.2 and 17.9%.

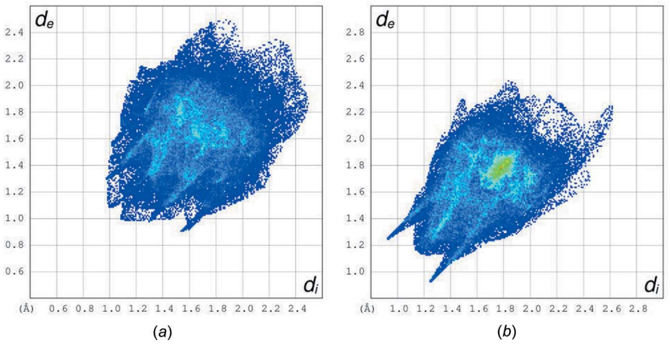

(*a*) (*b*)

Figure 7
FP plots for (*a*) [**4**: R = 3,4,5-(MeO)$_3$C$_6$H$_2$·0.5DMSO] and (*b*) (**4**: R = C$_6$H$_5$) in which the blue spikes ending at (1.2; 0.9) and (0.9;1.1) relate to O···H/H···O contacts and the high intensity of pixels, green and red areas relate to C···C contacts.

Table 4
Percentages for atom···atom close contacts.

Compound	[**4**: R = (3,4,5-MeO)$_3$C$_6$H$_2$·0.5DMSO]	(**4**: R = C$_6$H$_5$)
O···H/H···O	20.2	28.4
O···N/N···O	1.9	–
O···C/C···O	6.0	2.4
O···O	–	1.2
N···C/C···N	3.3	2.3
N···H/H···N	2.4	2.7
H···C/C···H	17.9	23.7
C···C	8.9	1.7
H···H	39.2	37.1

3.3. Lattice energy and intermolecular interaction energy calculations

Lattice energies and intermolecular interaction energies were calculated using the PIXEL routine implemented in the *CLP* package (Gavezzotti, 2003, 2008) which allows the calculation of intermolecular energies by distributed charge description on the basis of a preliminary evaluation of charge density from *GAUSSIAN* at the MP2/6-311G** level of theory (CUBE option). The PIXEL mode calculates the total stabilization energies of the crystal packing, $E_{\rm tot}$, distributed as coulombic, ($E_{\rm coul}$), polarization ($E_{\rm pol}$), dispersion ($E_{\rm disp}$) and repulsion ($E_{\rm rep}$) terms between separate, rigid molecules. Coulombic terms are treated on the basis of Coulombic law, polarization terms are calculated as a linear dipole approximation, dispersion terms are based on London's inverse six-power approximation involving ionization potentials and polarizabilities and the repulsion term comes from a modulated function of the wave-function overlap.

The presence of a half molecule of DMSO lying at a symmetry centre in [**4**: R = (3,4,5-MeO)$_3$C$_6$H$_2$·0.5DMSO], precludes the PIXEL analysis for this structure. Partial analysis of the PIXEL calculations, however, was carried out on (**4**: $R = C_6H_5$). The six molecule pairs that contribute most to the total energy of the packing of (**4**: $R = C_6H_5$) are shown in Fig. 8.

The various energies for these six significant molecule pairs are also listed in Fig. 8. As such energy values pertain to both the reference molecule at *x*, *y*, *z* and its partner in the molecule pair, the energies thus associated with the reference molecule at *x*, *y*, *z* are half of these sums. The total PIXEL energy calculated for the complete lattice is -157.9 kJ.mol^{-1}. Of that, -123.9 kJ.mol^{-1}(78.5%) is derived from the six molecule pairs shown in Fig. 8. The percentage contribution of pairs involved in O—H···O hydrogen bonds is 29.4% while pairs making C···C close contacts contribute 26.6% to the total stabilization energy.

4. Database survey

A search of the Cambridge Structural Database (CSD Version 5.39, August 2018 update; Groom *et al.*, 2016) found only one structure of type **4**, namely R = 4-MeOC$_6$H$_4$), which is currently undergoing enhancement with a current R value of

Pair no	Molecule pair	Symmetry code of molecule, in green, paired with that at x,y,z, molecule in element colours.	Other details	Calculated energies (kJ.mol^{-1})^a	
I	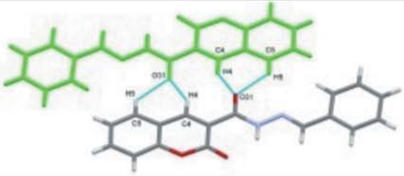	*2-x,-y,1-z*	Dimer formed form C5-H5-O31, O31---H5-C5, C4-H4---O31 and O31-H4-C4	E_{tot} E_{coul} E_{pol} E_{disp} E_{rep}	-60.2 -50.5 -20.0 -39.7 50.0
II III	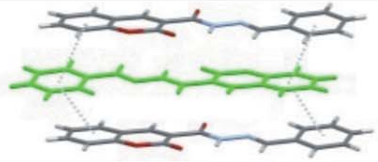	Pair II: i =*1-x,-y,1-z* Pair III: ii = *1-x,1-y, 1-z*	Formed from π---π^i π---π^{ii}	E_{tot} E_{coul} E_{pol} E_{disp} E_{rep}	Pair II and III -47.4 -36.6 -18.7 -4.9 -9.4 -5.9 -76.0 -68.4 56.7 42.6
VI	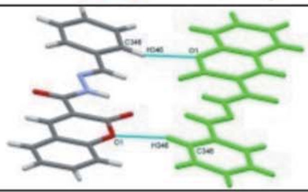	*-x,-y,1-z*	Dimer formed from C346-H346---O1 and C34-H34--O2	E_{tot} E_{coul} E_{pol} E_{disp} E_{rep}	-38.6 -26.0 -11.1 -41.2 39.6

Va Vb	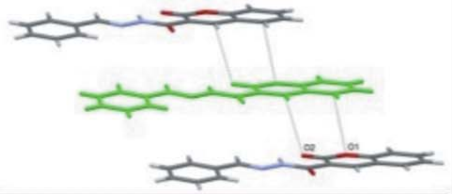	Pair Va : *1+x,y,z* Pair Vb : 1-*x,y,z*	Molecule pairs generated from the O2---C4 and O1---C5 close contacts	E_{tot} E_{coul} E_{pol} E_{disp} E_{rep}	Pair Va Vb -32.5 -32.5 -9.0 -9.0 -6.3 -6.3 -39.9 -39.8 22.6 22.6

^{a}: Energy of the interaction of the molecule-pairs, E_{tot}, distributed as Coulombic, (E_{coul}), polarization (E_{pol}), dispersion (E_{disp}) and repulsion (E_{rep})

Figure 8
Calculated energies for the most significant molecule pairs in (**4**: *R* = C_6H_5).

0.094 (Low & Wardell, 2019) and was briefly mentioned in a submitted article (Capelini *et al.*, 2019). The molecule of (**4**: *R* = 4-MeOC_6H_4) has a near-planar conformation and possesses equivalent intramolecular hydrogen bonds to those shown by the compounds reported in this article. A database search revealed other types of nitrogen-containing 2-oxo-2*H*-chromene derivatives, including amido derivatives (Gomes *et al.*, 2016*a*,*b*); see also: DOLYEK (Borges *et al.*, 2014*a*), DOLYIO (Cagide *et al.*, 2015) and DOLYOU (Borges *et al.*, 2014*b*, 2016). Angelova *et al.* (2017) reported the structures of (**1**: R^1 = Me, *R* = C_6H_5) and (**1**: R^1 = Me, *R* = pyridine-4-yl).

5. Synthesis and crystallization

5.1. General procedure for the synthesis of compounds 4

To a suspension of coumarinic acid (*cis-o*-hydroxycinammic acid, C_9H_3OH) (29 mmol, 1.0 equiv.) in CH_3CN (100 ml) at room temperature, was added HOBt (34.64 mmol, 1.2 equiv.), followed by EDC (65.40 mmol, 2.25 equiv). The reaction was stirred at room temperature for 2 h, and slowly added to a solution of hydrazine hydrate (58.20 mmol, 2.0 equiv.) in CH_3CN (100 mL) maintaining the temperature below 283 K. Water (70ml) was added to the reaction mixture, which was extracted successively with chloroform (3 × 95 mL) and aqueous 5% sodium bicarbonate (3 × 120 mL). The organic phases were collected and rotary evaporated to yield the coumarinic hydrazide (**5**), as a yellow solid. Crystallization of compound [**4**: *R* = (3,4,5-(MeO)$_3C_6H_2$] from DMSO solution produced the hemi-DMSO solvate, which on heating slowly decomposed to a dark residue. Attempts to gain suitable crystals for the structural study by slow recrystallization from ethanol solution at room temperature failed.

(*E*)-*N*'-Benzylidene-2-oxo-2*H*-chromene-3-carbohydrazide (4: *R* = C_6H_5). Yield: 78%. m.p. 403.7 K.

^{1}H NMR (400 MHz, DMSO-d_6) δ 7.48 (4H, *m*), 7.55 (1H, *d*, *J* = 8.32 Hz), 7.77 (3H, *m*), 8.02 [1H, *dd*, *J*(*o*) = 7.84 Hz, *J*(*m*) = 1.52 Hz], 8.47 (1H, *s*), 8.92 (1H, *s*) 11.76 (1H, *s*).

Table 5
Experimental details.

	[**4**: *R* = (3,4,5-MeO)$_3$C$_6$H$_2$·0.5DMSO]	(**4**: *R* = C$_6$H$_5$)
Crystal data		
Chemical formula	$C_{20}H_{18}N_2O_6 \cdot 0.5C_2H_6OS$	$C_{17}H_{12}N_2O_3$
M_r	421.43	292.29
Crystal system, space group	Monoclinic, *C*2/*c*	Triclinic, $P\overline{1}$
Temperature (K)	100	100
a, *b*, *c* (Å)	33.0258 (7), 5.4412 (1), 22.4342 (4)	5.6715 (1), 7.4164 (1), 15.9819 (3)
α, β, γ (°)	90, 107.203 (2), 90	88.369 (1), 84.147 (1), 82.961 (2)
V (Å^3)	3851.07 (13)	663.60 (2)
Z	8	2
Radiation type	Mo *K*α	Cu *K*α
μ (mm^{-1})	0.16	0.84
Crystal size (mm)	0.40 × 0.08 × 0.04	0.22 × 0.12 × 0.05
Data collection		
Diffractometer	Rigaku FRE+ equipped with VHF Varimax confocal mirrors and an AFC12 goniometer and HyPix 6000 detector	Rigaku 007HF equipped with Varimax confocal mirrors and an AFC11 goniometer and HyPix 6000 detector
Absorption correction	Gaussian (*CrysAlis PRO*; Rigaku OD, 2019)	Multi-scan (*CrysAlis PRO*; Rigaku OD, 2019)
T_{min}, T_{max}	0.837, 1.000	0.930, 1.000
No. of measured, independent and observed [$I > 2\sigma(I)$] reflections	22915, 4381, 3983	11641, 2352, 2250
R_{int}	0.016	0.027
(sin $\theta/\lambda)_{max}$ (Å^{-1})	0.649	0.597
Refinement		
$R[F^2 > 2\sigma(F^2)]$, $wR(F^2)$, *S*	0.032, 0.086, 1.05	0.033, 0.104, 0.88
No. of reflections	4381	2352
No. of parameters	298	203
H-atom treatment	H atoms treated by a mixture of independent and constrained refinement	H atoms treated by a mixture of independent and constrained refinement
$\Delta\rho_{max}$, $\Delta\rho_{min}$ (e Å^{-3})	0.31, −0.30	0.23, −0.19

Computer programs: *CrysAlis PRO* (Rigaku OD, 2019), *OSCAIL* (McArdle *et al.*, 2004), *SHELXT* (Sheldrick, 2015*a*), *ShelXle* (Hübschle *et al.*, 2011) *SHELXL2017* (Sheldrick, 2015*b*), *Mercury* (Macrae *et al.*, 2006), and *PLATON* (Spek, 2009).

^{13}C NMR (100 MHz, DMSO-*d*$_6$) *δ* 116.2, 118.4, 119.3, 125.3, 127.4, 128.9, 130.3, 130.4, 133.9, 134.3, 147.8, 149.4, 153.9, 158.1, 159.8.

EI/MS (*m*/*z*) [*M* + Na]$^+$: 315.11.

IR (KBr) ν_{max} cm^{-1}: 3216.34 (N—H, bonded), 3064.30 (C—H, *sp*^{2}), 1695.02 (C=O, lactone), 1663.15 (C=O, amide), 1604.10 (C=C, double bond coumarin), 1531.50 and 1488.69 (C=C, aromatic), 788 and 748 (monosubstituted aromatic).

To a solution of the coumarinic hydrazide (**5**) (0.98 mmol) in absolute ethanol (25 mL), containing a catalytic amount of 37% aq. hydrochloric acid, were added 1.03 mmol (1.05 equiv) of the desired benzaldehyde derivative. The mixture was refluxed until TLC indicated the complete consumption of **5** and the precipitate was collected and dried to yield the desired compound **4**, in yields ranging from 55 to 84%.

(*E*)-2-Oxo-*N*'-(3,4,5-trimethoxybenzylidene)-2*H*-chromene-3-carbohydrazide [4: *R* = (3,4,5-MeO)$_3$C$_6$H$_2$]. Yield: 76%. m.p. 368.7 K.

^{1}H NMR (400 MHz, DMSO-*d*$_6$) *δ* 3.72 (3H, *s*), 3.84 (6H, *s*), 7.08 (2H, *s*), 7.47 [1H, *t*, *J*(*o*) = 7.88 Hz, *J*(*m*) = 0.96 Hz], 7.55 [1H, *d*, *J*(*o*) = 8.36 Hz], 7.78 [1H, t, *J*(*o*) = 7.88 Hz, *J*(*m*) = 1.6 Hz], 8.02 [1H, *dd*, *J*(*o*) = 7.84 Hz, *J*(*m*) = 1.44 Hz], 8.38 (1H, *s*), 8.90 (1H, *s*), 11.74 (1H, *s*).

^{13}C NMR (100 MHz, DMSO-*d*$_6$)*δ* 55.8, 60.0, 104.5, 116.1, 118.3, 119.3, 125.2, 129.2, 130.2, 134.2, 139.4, 147.6, 149.3, 153.0, 153.8, 157.9, 159.8.

EI/MS (*m*/*z*) [*M* + H]$^+$: 383.13, **[*M* + Na]$^+$**: 405.09.

IR (KBr) ν_{max} cm^{-1}: 3185.12 (N—H), 2941.30 (C—H, *sp*^{3}), 1698.89 (C=O, lactone), 1666.73 (C=O, amide), 1609.91 (C=C, double bond coumarin), 1532.56 and 1499.88 (C=C, aromatic), 1229.99 and 1121.84 (C—O—C).

Suitable crystals of **4** for the structural study were obtained by slow evaporation of a solution in ethanol at room temperature

6. Refinement

Crystal data, data collection and structure refinement details are summarized in Table 5. C-bound H atoms were refined as riding atoms at calculated positions [C—H = 0.95–0.98 Å with U_{iso}(H) = 1.2–1.5U_{eq}(C)]. That attached to the N atom was refined.

In [**4**: *R* = 3,4,5-MeO$_3$C$_6$H$_2$·0.5DMSO] the solvent DMSO molecule lies on a crystallographic twofold axis. It was refined with a fixed occupancy factor of 0.5. A refinement of the s.o.f.

gave a value of 0.488. The DMSO molecules are located in channels which run along the twofold axis.

Acknowledgements

The authors thank the staff at the National Crystallographic Service, University of Southampton (Coles & Gale, 2012) for the data collection, help and advice.

References

Angelova, V. T., Valcheva, V., Vassilev, N. G., Buyukliev, R., Momekov, G., Dimitrov, I., Saso, L., Djukic, M. & Shivachev, B. (2017). *Bioorg. Med. Chem. Lett.* **27**, 223–227.

Borges, F., Gomes, L. R. & Low, J. N. (2014*a*). Private Communication (refcode DOLYEK). CCDC, Cambridge, England.

Borges, F., Gomes, L. R. & Low, J. N. (2014*b*). Private Communication (refcode DOLYOU). CCDC, Cambridge, England.

Borges, F., Gomes, L. R. & Low, J. N. (2016). Private Communication (refcode DOLYOU01). CCDC, Cambridge, England.

Cagide, F., Silva, T., Reis, J., Gaspar, A., Borges, F., Gomes, L. R. & Low, J. N. (2015). *Chem. Commun.* **51**, 2832–2835.

Capelini, C., Câmara, V. R. F., Figueroa Villar, J. D., Barbosa, J. M. C., Salomão, K., de Castro, S. L., Sales Junior, P. A., Murta, S. M. F., Couto, T. B., Lourenço, M. C. S., Wardell, J. L., Low, J. N., da Silva, E. D. F. & Carvalho, S. A. (2019). *Med. Chem*. Submitted.

Cardoso, S. H., Barreto, M. B., Lourenço, M. C. S., Henriques, M. das G. M. de O., Candéa, A. L. P., Kaiser, C. R. & de Souza, M. V. N. (2011). *Chem. Biol. Drug Des.* **77**, 489–493.

Coles, S. J. & Gale, P. A. (2012). *Chem. Sci.* **3**, 683–689.

Fraga, C. A. M. & Barreiro, E. J. (2006). *Curr. Med. Chem.* **13**, 167–198.

Gavezzotti, A. (2003). *J. Phys. Chem. B*, **107**, 2344–2353.

Gavezzotti, A. (2008). *Mol. Phys.* **106**, 1473–1485.

Gomes, L. R., Low, J. N., Fonseca, A., Matos, M. J. & Borges, F. (2016*a*). *Acta Cryst.* E**72**, 926–932.

Gomes, L. R., Low, J. N., Oliveira, C., Cagide, F. & Borges, F. (2016*b*). *Acta Cryst.* E**72**, 675–682.

Groom, C. R., Bruno, I. J., Lightfoot, M. P. & Ward, S. C. (2016). *Acta Cryst.* B**72**, 171–179.

Howie, R. A., da Silva Lima, C. H., Kaiser, C. R., de Souza, M. V. N., Wardell, J. L. & Wardell, S. M. S. V. (2010). *Z. Kristallogr.* **225**, 158–166.

Hübschle, C. B., Sheldrick, G. M. & Dittrich, B. (2011). *J. Appl. Cryst.* **44**, 1281–1284.

Low, J. N. & Wardell, J. (2019). Private Communication (CCDC 1914876). CCDC, Cambridge, England. doi: 10.5517/ccdc. csd. cc228l65.

Macrae, C. F., Edgington, P. R., McCabe, P., Pidcock, E., Shields, G. P., Taylor, R., Towler, M. & van de Streek, J. (2006). *J. Appl. Cryst.* **39**, 453–457.

McArdle, P., Gilligan, K., Cunningham, D., Dark, R. & Mahon, M. (2004). *CrystEngComm.* **6**, 303–309.

Peralta, M. A., de Souza, M. N. V., Wardell, S. M. S. V., Wardell, J. L., Low, J. N. & Glidewell, C. (2007). *Acta Cryst.* C**63**, o68–o72.

Rigaku OD (2019). *CryAlis PRO*. Rigaku Corporation, Tokyo, Japan.

Sheldrick, G. M. (2015*a*). *Acta Cryst.* A**71**, 3–8.

Sheldrick, G. M. (2015*b*). *Acta Cryst.* C**71**, 3–8.

Singh, N., Ranjana, R., Kumari, M. & Kumar, B. (2016). *Int. J. Pharm. Clin. Res.* **8**, 162-166.

Souza, S. P., Masteloto, H. G., da Silva, D. S., Azambuja, J. H., Braganhol, E., Ribeiro, J. S., Lund, R. G. & Cunico, W. (2017). *Lett. Drug. Des. & Discov*. **14**, 678–685.

Spackman, M. A. & Jayatilaka, D. (2009). *CrystEngComm*, **11**, 19–32.

Spackman, M. A. & McKinnon, J. J. (2002). *CrystEngComm*, **4**, 378–392.

Spek, A. L. (2009). *Acta Cryst.* D**65**, 148–155.

Wolff, S. K., Grimwood, D. I., McKinnon, J. J., Turner, M. J., Jayatilaka, D. & Spackman, M. A. (2012). *Crystal Explorer*. The University of Western Australia.

supporting information

Acta Cryst. (2019). E**75**, 1403-1410   [https://doi.org/10.1107/S2056989019012015]

Crystal structures and Hirshfeld surface analyses of (*E*)-*N*′-benzylidene-2-oxo-2*H*-chromene-3-carbohydrazide and the disordered hemi-DMSO solvate of (*E*)-2-oxo-*N*′-(3,4,5-trimethoxybenzylidene)-2*H*-chromene-3-carbohydrazide: lattice energy and intermolecular interaction energy calculations for the latter

Ligia R. Gomes, John Nicolson Low, James L. Wardell, Camiola Capelini, Vitoria R.F. Câmara, Edson F. da Silva and Samir A. Carvalho

Computing details

For both structures, data collection: *CrysAlis PRO* (Rigaku OD, 2019); cell refinement: *CrysAlis PRO* (Rigaku OD, 2019); data reduction: *CrysAlis PRO* (Rigaku OD, 2019); program(s) used to solve structure: *OSCAIL* (McArdle *et al.*, 2004), SHELXT (Sheldrick, 2015a); program(s) used to refine structure: *OSCAIL* (McArdle *et al.*, 2004), *ShelXle* (Hübschle *et al.*, 2011) *SHELXL2017* (Sheldrick, 2015b); molecular graphics: *Mercury* (Macrae *et al.*, 2006). Software used to prepare material for publication: *OSCAIL* (McArdle *et al.*, 2004), *SHELXL2017* (Sheldrick, 2015b) *PLATON* (Spek, 2009) for (I); *OSCAIL* (McArdle *et al.*, 2004), *SHELX2017*/1 (Sheldrick, 2015b) *PLATON* (Spek, 2009) for (II).

(*E*)-2-Oxo-*N*′-(3,4,5-trimethoxybenzylidene)-2*H*-chromene-3-carbohydrazide dimethyl sulfoxide hemisolvate (I)

Crystal data

$C_{20}H_{18}N_2O_6 \cdot 0.5C_2H_6OS$
$M_r = 421.43$
Monoclinic, *C*2/*c*
$a = 33.0258$ (7) Å
$b = 5.4412$ (1) Å
$c = 22.4342$ (4) Å
$\beta = 107.203$ (2)°
$V = 3851.07$ (13) Å^3
$Z = 8$
$F(000) = 1768$
$D_x = 1.454$ Mg m^{-3}
Mo $K\alpha$ radiation, $\lambda = 0.71075$ Å
Cell parameters from 13857 reflections
$\theta = 2.0$–31.6°
$\mu = 0.16$ mm^{-1}
$T = 100$ K
Block, yellow
0.40 × 0.08 × 0.04 mm

Data collection

Rigaku FRE+ equipped with VHF Varimax confocal mirrors and an AFC12 goniometer and HyPix 6000 detector diffractometer
Radiation source: Rotating Anode, Rigaku FRE+
Confocal mirrors, VHF Varimax monochromator
Detector resolution: 10 pixels mm^{-1}
profile data from ω–scans
Absorption correction: gaussian (CrysAlisPro; Rigaku OD, 2019)
$T_{min} = 0.837$, $T_{max} = 1.000$
22915 measured reflections
4381 independent reflections
3983 reflections with $I > 2\sigma(I)$
$R_{int} = 0.016$
$\theta_{max} = 27.5°$, $\theta_{min} = 2.6°$
$h = -42 \rightarrow 42$
$k = -6 \rightarrow 7$
$l = -26 \rightarrow 29$

Refinement

Refinement on F^2
Least-squares matrix: full
$R[F^2 > 2\sigma(F^2)] = 0.032$
$wR(F^2) = 0.086$
$S = 1.05$
4381 reflections
298 parameters
0 restraints
Hydrogen site location: mixed
H atoms treated by a mixture of independent and constrained refinement
$w = 1/[\sigma^2(F_o^2) + (0.0456P)^2 + 2.9167P]$ where $P = (F_o^2 + 2F_c^2)/3$
$(\Delta/\sigma)_{\max} = 0.001$
$\Delta\rho_{\max} = 0.31$ e Å^{-3}
$\Delta\rho_{\min} = -0.30$ e Å^{-3}

Special details

Geometry. All esds (except the esd in the dihedral angle between two l.s. planes) are estimated using the full covariance matrix. The cell esds are taken into account individually in the estimation of esds in distances, angles and torsion angles; correlations between esds in cell parameters are only used when they are defined by crystal symmetry. An approximate (isotropic) treatment of cell esds is used for estimating esds involving l.s. planes.

Fractional atomic coordinates and isotropic or equivalent isotropic displacement parameters (Å^2)

	x	*y*	*z*	$U_{\rm iso}$*/$U_{\rm eq}$	Occ. (<1)
O1	0.40457 (2)	0.68439 (13)	0.52398 (3)	0.01627 (16)	
O2	0.46021 (2)	0.81610 (14)	0.59671 (4)	0.02005 (17)	
O31	0.53178 (2)	0.20068 (14)	0.57120 (3)	0.01931 (17)	
O343	0.72470 (2)	0.31586 (14)	0.80720 (3)	0.01717 (16)	
O344	0.73938 (2)	0.64983 (14)	0.89856 (3)	0.01614 (16)	
O345	0.67832 (2)	0.95654 (15)	0.90901 (3)	0.02104 (17)	
N32	0.53224 (3)	0.55236 (18)	0.62643 (4)	0.01798 (19)	
H32	0.5171 (5)	0.679 (3)	0.6305 (7)	0.029 (4)*	
N33	0.57200 (3)	0.51012 (17)	0.66718 (4)	0.01668 (18)	
C2	0.44611 (3)	0.65614 (18)	0.55853 (4)	0.01415 (19)	
C3	0.46844 (3)	0.43809 (18)	0.54634 (4)	0.01325 (19)	
C4	0.44791 (3)	0.27552 (19)	0.50194 (4)	0.01369 (19)	
H4	0.462640	0.135045	0.494099	0.016*	
C5	0.38134 (3)	0.14563 (19)	0.42087 (5)	0.0175 (2)	
H5	0.394775	0.003909	0.410755	0.021*	
C4A	0.40442 (3)	0.31084 (18)	0.46651 (4)	0.01345 (19)	
C6	0.33896 (3)	0.1903 (2)	0.39072 (5)	0.0204 (2)	
H6	0.323245	0.077292	0.360352	0.024*	
C7	0.31911 (3)	0.4001 (2)	0.40457 (5)	0.0194 (2)	
H7	0.289997	0.428309	0.383493	0.023*	
C8	0.34135 (3)	0.5677 (2)	0.44868 (5)	0.0173 (2)	
H8	0.328020	0.711508	0.457860	0.021*	
C8A	0.38373 (3)	0.51893 (18)	0.47906 (4)	0.01401 (19)	
C31	0.51385 (3)	0.38442 (19)	0.58215 (4)	0.0144 (2)	
C34	0.58354 (3)	0.6722 (2)	0.70991 (5)	0.0234 (2)	
H34	0.565334	0.807515	0.709773	0.028*	
C341	0.62400 (3)	0.6560 (2)	0.75915 (5)	0.0182 (2)	
C342	0.65468 (3)	0.48341 (19)	0.75655 (4)	0.0154 (2)	
H342	0.649709	0.371929	0.722555	0.018*	
C343	0.69263 (3)	0.47723 (18)	0.80448 (4)	0.01379 (19)	

C344	0.70034 (3)	0.64402 (19)	0.85427 (4)	0.0140 (2)	
C345	0.66880 (3)	0.80974 (19)	0.85746 (5)	0.0165 (2)	
C346	0.63073 (3)	0.8169 (2)	0.80957 (5)	0.0207 (2)	
H346	0.609346	0.931306	0.811211	0.025*	
C431	0.71732 (4)	0.1389 (2)	0.75813 (5)	0.0207 (2)	
H43A	0.712251	0.223812	0.718061	0.031*	
H43B	0.692471	0.039486	0.757575	0.031*	
H43C	0.742175	0.032094	0.765084	0.031*	
C441	0.74230 (3)	0.4860 (2)	0.94982 (5)	0.0195 (2)	
H41A	0.736607	0.317514	0.934155	0.029*	
H41B	0.721429	0.533664	0.970960	0.029*	
H41C	0.770842	0.495051	0.979338	0.029*	
C451	0.64624 (3)	1.1251 (2)	0.91407 (5)	0.0196 (2)	
H51A	0.620280	1.034335	0.912316	0.029*	
H51B	0.640421	1.242953	0.879538	0.029*	
H51C	0.656046	1.213390	0.953827	0.029*	
S1S	0.50726 (2)	1.12167 (9)	0.72755 (2)	0.01665 (11)	0.5
O1S	0.4985 (16)	0.8678 (3)	0.7444 (12)	0.026 (2)	0.5
C1S	0.45886 (14)	1.2893 (14)	0.7013 (3)	0.0207 (9)	0.5
H1SA	0.442339	1.228493	0.660195	0.031*	0.5
H1SB	0.465103	1.464184	0.698321	0.031*	0.5
H1SC	0.442536	1.267478	0.730985	0.031*	0.5
C2S	0.52800 (15)	1.2784 (15)	0.7996 (3)	0.0300 (12)	0.5
H2SA	0.510606	1.241255	0.827053	0.045*	0.5
H2SB	0.527643	1.455833	0.791972	0.045*	0.5
H2SC	0.557203	1.224526	0.819443	0.045*	0.5

Atomic displacement parameters (Å^2)

	U^{11}	U^{22}	U^{33}	U^{12}	U^{13}	U^{23}
O1	0.0125 (3)	0.0167 (4)	0.0169 (3)	0.0020 (3)	0.0002 (3)	−0.0032 (3)
O2	0.0179 (4)	0.0181 (4)	0.0202 (4)	0.0021 (3)	−0.0004 (3)	−0.0066 (3)
O31	0.0143 (3)	0.0207 (4)	0.0198 (4)	0.0040 (3)	0.0002 (3)	−0.0052 (3)
O343	0.0150 (3)	0.0195 (4)	0.0151 (3)	0.0036 (3)	0.0015 (3)	−0.0017 (3)
O344	0.0122 (3)	0.0200 (4)	0.0129 (3)	−0.0033 (3)	−0.0014 (3)	0.0018 (3)
O345	0.0171 (4)	0.0253 (4)	0.0179 (4)	0.0004 (3)	0.0008 (3)	−0.0105 (3)
N32	0.0103 (4)	0.0222 (5)	0.0177 (4)	0.0040 (3)	−0.0017 (3)	−0.0063 (3)
N33	0.0104 (4)	0.0231 (5)	0.0144 (4)	0.0001 (3)	0.0003 (3)	−0.0022 (3)
C2	0.0122 (4)	0.0160 (5)	0.0130 (4)	0.0007 (4)	0.0018 (3)	0.0001 (4)
C3	0.0115 (4)	0.0149 (5)	0.0124 (4)	0.0008 (4)	0.0022 (3)	0.0002 (4)
C4	0.0135 (4)	0.0140 (5)	0.0130 (4)	0.0007 (4)	0.0031 (4)	0.0006 (4)
C5	0.0183 (5)	0.0165 (5)	0.0156 (5)	−0.0020 (4)	0.0018 (4)	−0.0006 (4)
C4A	0.0129 (4)	0.0147 (5)	0.0117 (4)	−0.0013 (4)	0.0021 (3)	0.0015 (3)
C6	0.0189 (5)	0.0223 (5)	0.0155 (5)	−0.0060 (4)	−0.0020 (4)	−0.0002 (4)
C7	0.0124 (5)	0.0248 (6)	0.0171 (5)	−0.0022 (4)	−0.0015 (4)	0.0060 (4)
C8	0.0139 (5)	0.0186 (5)	0.0183 (5)	0.0016 (4)	0.0031 (4)	0.0042 (4)
C8A	0.0135 (4)	0.0148 (5)	0.0125 (4)	−0.0021 (4)	0.0020 (4)	0.0008 (4)
C31	0.0119 (4)	0.0179 (5)	0.0123 (4)	0.0003 (4)	0.0019 (3)	−0.0009 (4)

C34	0.0143 (5)	0.0289 (6)	0.0226 (5)	0.0051 (4)	−0.0011 (4)	−0.0099 (4)
C341	0.0131 (5)	0.0229 (5)	0.0163 (5)	−0.0007 (4)	0.0008 (4)	−0.0050 (4)
C342	0.0142 (4)	0.0188 (5)	0.0122 (4)	−0.0016 (4)	0.0024 (4)	−0.0034 (4)
C343	0.0132 (4)	0.0151 (5)	0.0136 (4)	−0.0005 (4)	0.0047 (4)	0.0014 (4)
C344	0.0109 (4)	0.0177 (5)	0.0116 (4)	−0.0032 (4)	0.0007 (3)	0.0010 (4)
C345	0.0157 (5)	0.0191 (5)	0.0137 (5)	−0.0032 (4)	0.0031 (4)	−0.0049 (4)
C346	0.0140 (5)	0.0250 (6)	0.0209 (5)	0.0029 (4)	0.0019 (4)	−0.0081 (4)
C431	0.0224 (5)	0.0185 (5)	0.0203 (5)	0.0032 (4)	0.0051 (4)	−0.0037 (4)
C441	0.0193 (5)	0.0220 (5)	0.0145 (5)	−0.0009 (4)	0.0007 (4)	0.0032 (4)
C451	0.0180 (5)	0.0209 (5)	0.0205 (5)	−0.0021 (4)	0.0064 (4)	−0.0075 (4)
S1S	0.0182 (2)	0.0149 (2)	0.0183 (2)	0.00064 (18)	0.00770 (19)	−0.00093 (19)
O1S	0.040 (5)	0.0140 (6)	0.030 (7)	0.0000 (17)	0.020 (7)	−0.0005 (12)
C1S	0.019 (2)	0.0187 (14)	0.0218 (14)	0.003 (2)	0.0018 (17)	0.0027 (10)
C2S	0.033 (3)	0.024 (2)	0.0284 (17)	0.006 (3)	0.001 (2)	−0.0054 (13)

Geometric parameters (Å, º)

O1—C2	1.3702 (12)	C34—C341	1.4629 (14)
O1—C8A	1.3747 (12)	C34—H34	0.9500
O2—C2	1.2133 (12)	C341—C342	1.3953 (14)
O31—C31	1.2234 (13)	C341—C346	1.3955 (14)
O343—C343	1.3631 (12)	C342—C343	1.3894 (13)
O343—C431	1.4280 (12)	C342—H342	0.9500
O344—C344	1.3759 (11)	C343—C344	1.4028 (14)
O344—C441	1.4356 (12)	C344—C345	1.3955 (14)
O345—C345	1.3635 (12)	C345—C346	1.3921 (14)
O345—C451	1.4309 (13)	C346—H346	0.9500
N32—C31	1.3543 (13)	C431—H43A	0.9800
N32—N33	1.3793 (11)	C431—H43B	0.9800
N32—H32	0.870 (16)	C431—H43C	0.9800
N33—C34	1.2753 (14)	C441—H41A	0.9800
C2—C3	1.4647 (13)	C441—H41B	0.9800
C3—C4	1.3547 (14)	C441—H41C	0.9800
C3—C31	1.5056 (13)	C451—H51A	0.9800
C4—C4A	1.4340 (13)	C451—H51B	0.9800
C4—H4	0.9500	C451—H51C	0.9800
C5—C6	1.3840 (15)	S1S—O1S	1.483 (16)
C5—C4A	1.4057 (14)	S1S—C2S	1.775 (7)
C5—H5	0.9500	S1S—C1S	1.782 (5)
C4A—C8A	1.3935 (14)	C1S—H1SA	0.9800
C6—C7	1.3965 (16)	C1S—H1SB	0.9800
C6—H6	0.9500	C1S—H1SC	0.9800
C7—C8	1.3856 (15)	C2S—H2SA	0.9800
C7—H7	0.9500	C2S—H2SB	0.9800
C8—C8A	1.3890 (13)	C2S—H2SC	0.9800
C8—H8	0.9500		
C2—O1—C8A	122.80 (8)	C341—C342—H342	120.5

C343—O343—C431	116.52 (8)	O343—C343—C342	124.14 (9)
C344—O344—C441	113.00 (8)	O343—C343—C344	115.17 (8)
C345—O345—C451	116.90 (8)	C342—C343—C344	120.69 (9)
C31—N32—N33	120.41 (9)	O344—C344—C345	120.16 (9)
C31—N32—H32	117.6 (10)	O344—C344—C343	120.05 (9)
N33—N32—H32	121.7 (10)	C345—C344—C343	119.76 (9)
C34—N33—N32	113.41 (9)	O345—C345—C346	124.54 (9)
O2—C2—O1	115.46 (9)	O345—C345—C344	115.71 (9)
O2—C2—C3	127.12 (9)	C346—C345—C344	119.75 (9)
O1—C2—C3	117.42 (8)	C345—C346—C341	119.92 (10)
C4—C3—C2	119.74 (9)	C345—C346—H346	120.0
C4—C3—C31	117.95 (9)	C341—C346—H346	120.0
C2—C3—C31	122.31 (9)	O343—C431—H43A	109.5
C3—C4—C4A	121.44 (9)	O343—C431—H43B	109.5
C3—C4—H4	119.3	H43A—C431—H43B	109.5
C4A—C4—H4	119.3	O343—C431—H43C	109.5
C6—C5—C4A	119.72 (10)	H43A—C431—H43C	109.5
C6—C5—H5	120.1	H43B—C431—H43C	109.5
C4A—C5—H5	120.1	O344—C441—H41A	109.5
C8A—C4A—C5	118.30 (9)	O344—C441—H41B	109.5
C8A—C4A—C4	117.88 (9)	H41A—C441—H41B	109.5
C5—C4A—C4	123.81 (9)	O344—C441—H41C	109.5
C5—C6—C7	120.56 (10)	H41A—C441—H41C	109.5
C5—C6—H6	119.7	H41B—C441—H41C	109.5
C7—C6—H6	119.7	O345—C451—H51A	109.5
C8—C7—C6	120.80 (9)	O345—C451—H51B	109.5
C8—C7—H7	119.6	H51A—C451—H51B	109.5
C6—C7—H7	119.6	O345—C451—H51C	109.5
C7—C8—C8A	117.99 (10)	H51A—C451—H51C	109.5
C7—C8—H8	121.0	H51B—C451—H51C	109.5
C8A—C8—H8	121.0	O1S—S1S—C2S	105.5 (10)
O1—C8A—C8	116.63 (9)	O1S—S1S—C1S	109.8 (19)
O1—C8A—C4A	120.73 (9)	C2S—S1S—C1S	96.99 (18)
C8—C8A—C4A	122.62 (9)	S1S—C1S—H1SA	109.5
O31—C31—N32	124.05 (9)	S1S—C1S—H1SB	109.5
O31—C31—C3	121.09 (9)	H1SA—C1S—H1SB	109.5
N32—C31—C3	114.86 (9)	S1S—C1S—H1SC	109.5
N33—C34—C341	121.94 (10)	H1SA—C1S—H1SC	109.5
N33—C34—H34	119.0	H1SB—C1S—H1SC	109.5
C341—C34—H34	119.0	S1S—C2S—H2SA	109.5
C342—C341—C346	120.85 (9)	S1S—C2S—H2SB	109.5
C342—C341—C34	121.44 (9)	H2SA—C2S—H2SB	109.5
C346—C341—C34	117.71 (9)	S1S—C2S—H2SC	109.5
C343—C342—C341	118.94 (9)	H2SA—C2S—H2SC	109.5
C343—C342—H342	120.5	H2SB—C2S—H2SC	109.5

C31—N32—N33—C34	−173.67 (10)	C4—C3—C31—N32	−179.03 (9)
C8A—O1—C2—O2	−179.61 (9)	C2—C3—C31—N32	0.25 (14)

C8A—O1—C2—C3	−0.32 (13)	N32—N33—C34—C341	177.68 (10)
O2—C2—C3—C4	179.69 (10)	N33—C34—C341—C342	9.81 (18)
O1—C2—C3—C4	0.50 (14)	N33—C34—C341—C346	−169.23 (11)
O2—C2—C3—C31	0.42 (16)	C346—C341—C342—C343	−1.33 (16)
O1—C2—C3—C31	−178.77 (8)	C34—C341—C342—C343	179.66 (10)
C2—C3—C4—C4A	−0.40 (14)	C431—O343—C343—C342	−2.19 (14)
C31—C3—C4—C4A	178.90 (9)	C431—O343—C343—C344	178.22 (9)
C6—C5—C4A—C8A	−1.25 (15)	C341—C342—C343—O343	179.45 (9)
C6—C5—C4A—C4	177.48 (9)	C341—C342—C343—C344	−0.98 (15)
C3—C4—C4A—C8A	0.11 (14)	C441—O344—C344—C345	92.74 (11)
C3—C4—C4A—C5	−178.62 (9)	C441—O344—C344—C343	−89.56 (11)
C4A—C5—C6—C7	1.01 (16)	O343—C343—C344—O344	5.20 (13)
C5—C6—C7—C8	0.00 (16)	C342—C343—C344—O344	−174.41 (9)
C6—C7—C8—C8A	−0.72 (15)	O343—C343—C344—C345	−177.09 (9)
C2—O1—C8A—C8	178.49 (9)	C342—C343—C344—C345	3.30 (15)
C2—O1—C8A—C4A	0.04 (14)	C451—O345—C345—C346	1.34 (15)
C7—C8—C8A—O1	−177.96 (9)	C451—O345—C345—C344	−178.86 (9)
C7—C8—C8A—C4A	0.46 (15)	O344—C344—C345—O345	−5.41 (14)
C5—C4A—C8A—O1	178.88 (9)	C343—C344—C345—O345	176.88 (9)
C4—C4A—C8A—O1	0.08 (14)	O344—C344—C345—C346	174.40 (9)
C5—C4A—C8A—C8	0.52 (15)	C343—C344—C345—C346	−3.31 (15)
C4—C4A—C8A—C8	−178.28 (9)	O345—C345—C346—C341	−179.17 (10)
N33—N32—C31—O31	−7.04 (16)	C344—C345—C346—C341	1.03 (17)
N33—N32—C31—C3	172.52 (8)	C342—C341—C346—C345	1.31 (17)
C4—C3—C31—O31	0.54 (14)	C34—C341—C346—C345	−179.64 (10)
C2—C3—C31—O31	179.82 (9)		

Hydrogen-bond geometry (Å, º)

*Cg*1, *Cg*2 and *Cg*3 are the centroids of the O1/C2–C4/C4*A*/C8*A*, C4*A*/C5–C8/C8*A* and C341–C346 rings, respectively.

D—H···*A*	*D*—H	H···*A*	*D*···*A*	*D*—H···*A*
N32—H32···O2	0.870 (16)	1.955 (15)	2.6878 (12)	141.0 (14)
C441—H41*C*···O345^{i}	0.98	2.58	3.4772 (12)	152
C451—H51*A*···O1^{ii}	0.98	2.65	3.4463 (13)	138
C34—H34···O1*S*	0.95	2.57	3.30 (5)	134
C34—H34···O1*S*^{ii}	0.95	2.63	3.34 (5)	133
C34—H34···S1*S*	0.95	2.69	3.6158 (12)	166
C431—H43*C*···O343^{iii}	0.98	2.50	3.2505 (13)	133
C2*S*—H2*SA*···N32^{iv}	0.98	2.61	3.3000 (6)	127
C4—H4···O31	0.95	2.45	2.7761 (12)	100
C4—H4···O31^{v}	0.95	2.38	3.2415 (12)	150
C5—H5···O31^{v}	0.95	2.59	3.3931 (13)	143
C431—H43*B*···*Cg*3^{vi}	0.98	2.73	3.5882 (13)	147
C451—H51*B*···*Cg*3^{vi}	0.98	2.95	3.8562 (12)	155
C451—H51*C*···*Cg*2^{vii}	0.98	2.83	3.6883 (13)	147
C31—O31···*Cg*1^{vii}	0	0	3.3971 (6)	90 (1)

Symmetry codes: (i) $-x+3/2, -y+3/2, -z+2$; (ii) $-x+1, y, -z+3/2$; (iii) $-x+3/2, y-1/2, -z+3/2$; (iv) $-x+1, y+1, -z+3/2$; (v) $-x+1, -y, -z+1$; (vi) $x, y-1, z$; (vii) $-x+1, -y+1, -z+1$.

(*E*)-*N*′-Benzylidene-2-oxo-2*H*-chromene-3-carbohydrazide (II)

Crystal data

$C_{17}H_{12}N_2O_3$
$M_r = 292.29$
Triclinic, $P\overline{1}$
$a = 5.6715$ (1) Å
$b = 7.4164$ (1) Å
$c = 15.9819$ (3) Å
$\alpha = 88.369$ (1)°
$\beta = 84.147$ (1)°
$\gamma = 82.961$ (2)°
$V = 663.60$ (2) Å^3

$Z = 2$
$F(000) = 304$
$D_x = 1.463$ Mg m^{-3}
Cu $K\alpha$ radiation, $\lambda = 1.54178$ Å
Cell parameters from 8290 reflections
$\theta = 6.0$–70.3°
$\mu = 0.84$ mm^{-1}
$T = 100$ K
Plate, colourless
0.22 × 0.12 × 0.05 mm

Data collection

Rigaku 007HF equipped with Varimax confocal mirrors and an AFC11 goniometer and HyPix 6000 detector diffractometer
Radiation source: Rotating anode, Rigaku 007 HF
Varimax focusing mirrors monochromator
Detector resolution: 10 pixels mm^{-1}
profile data from ω–scans

Absorption correction: multi-scan (CrysAlisPro; Rigaku OD, 2019)
$T_{\min} = 0.930$, $T_{\max} = 1.000$
11641 measured reflections
2352 independent reflections
2250 reflections with $I > 2\sigma(I)$
$R_{\text{int}} = 0.027$
$\theta_{\max} = 67.1°$, $\theta_{\min} = 5.6°$
$h = -6 \rightarrow 6$
$k = -8 \rightarrow 8$
$l = -19 \rightarrow 19$

Refinement

Refinement on F^2
Least-squares matrix: full
$R[F^2 > 2\sigma(F^2)] = 0.033$
$wR(F^2) = 0.104$
$S = 0.88$
2352 reflections
203 parameters
0 restraints

Hydrogen site location: mixed
H atoms treated by a mixture of independent and constrained refinement
$w = 1/[\sigma^2(F_o^2) + (0.0858P)^2 + 0.127P]$ where $P = (F_o^2 + 2F_c^2)/3$
$(\Delta/\sigma)_{\max} = 0.001$
$\Delta\rho_{\max} = 0.23$ e Å^{-3}
$\Delta\rho_{\min} = -0.19$ e Å^{-3}

Special details

Geometry. All esds (except the esd in the dihedral angle between two l.s. planes) are estimated using the full covariance matrix. The cell esds are taken into account individually in the estimation of esds in distances, angles and torsion angles; correlations between esds in cell parameters are only used when they are defined by crystal symmetry. An approximate (isotropic) treatment of cell esds is used for estimating esds involving l.s. planes.

Fractional atomic coordinates and isotropic or equivalent isotropic displacement parameters (Å^2)

	x	y	z	U_{iso}*/U_{eq}
O1	0.38486 (11)	0.36429 (9)	0.68964 (4)	0.0233 (2)
H1	0.276 (3)	0.3194 (18)	0.4545 (9)	0.043 (4)*
O2	0.19764 (11)	0.41255 (9)	0.57568 (4)	0.0256 (2)
O31	0.77445 (12)	0.11739 (10)	0.43121 (4)	0.0316 (2)
N32	0.40134 (15)	0.26503 (11)	0.42751 (5)	0.0220 (2)
N33	0.40966 (14)	0.23814 (10)	0.34233 (5)	0.0227 (2)
C2	0.37588 (16)	0.34215 (12)	0.60485 (6)	0.0213 (2)

C3	0.58217 (17)	0.23662 (12)	0.55958 (6)	0.0213 (2)
C4	0.76971 (17)	0.16687 (12)	0.60074 (6)	0.0223 (2)
H4	0.9026	0.0993	0.5703	0.027*
C5	0.96435 (17)	0.12171 (13)	0.73471 (6)	0.0240 (2)
H5	1.1005	0.0524	0.7070	0.029*
C4A	0.77384 (17)	0.19200 (12)	0.68915 (6)	0.0217 (2)
C6	0.95376 (17)	0.15324 (13)	0.81971 (6)	0.0256 (2)
H6	1.0835	0.1068	0.8504	0.031*
C7	0.75272 (18)	0.25331 (13)	0.86075 (6)	0.0264 (2)
H7	0.7472	0.2744	0.9193	0.032*
C8	0.56165 (18)	0.32215 (13)	0.81749 (6)	0.0251 (2)
H8	0.4243	0.3888	0.8458	0.030*
C8A	0.57482 (17)	0.29175 (12)	0.73184 (6)	0.0219 (2)
C31	0.59517 (17)	0.20132 (12)	0.46715 (6)	0.0232 (2)
C34	0.22002 (17)	0.29462 (12)	0.30817 (6)	0.0216 (2)
H34	0.0821	0.3485	0.3413	0.026*
C341	0.21746 (16)	0.27545 (12)	0.21730 (6)	0.0215 (2)
C342	0.41939 (17)	0.19665 (13)	0.16727 (6)	0.0238 (2)
H342	0.5605	0.1523	0.1923	0.029*
C343	0.41260 (17)	0.18368 (13)	0.08144 (6)	0.0274 (2)
H343	0.5495	0.1299	0.0478	0.033*
C344	0.20758 (19)	0.24849 (14)	0.04380 (6)	0.0289 (2)
H344	0.2048	0.2399	−0.0153	0.035*
C345	0.00689 (18)	0.32579 (14)	0.09316 (6)	0.0280 (2)
H345	−0.1337	0.3703	0.0678	0.034*
C346	0.01167 (17)	0.33801 (13)	0.17960 (6)	0.0249 (2)
H346	−0.1267	0.3895	0.2132	0.030*

Atomic displacement parameters ($Å^2$)

	U^{11}	U^{22}	U^{33}	U^{12}	U^{13}	U^{23}
O1	0.0226 (4)	0.0284 (4)	0.0176 (4)	0.0025 (3)	−0.0017 (3)	−0.0030 (3)
O2	0.0214 (4)	0.0315 (4)	0.0223 (4)	0.0050 (3)	−0.0029 (3)	−0.0030 (3)
O31	0.0276 (4)	0.0432 (4)	0.0196 (4)	0.0139 (3)	−0.0021 (3)	−0.0048 (3)
N32	0.0215 (4)	0.0275 (4)	0.0155 (4)	0.0034 (3)	−0.0008 (3)	−0.0034 (3)
N33	0.0251 (4)	0.0257 (4)	0.0165 (4)	0.0002 (3)	−0.0014 (3)	−0.0022 (3)
C2	0.0229 (5)	0.0227 (5)	0.0181 (5)	−0.0016 (4)	−0.0014 (4)	−0.0013 (3)
C3	0.0215 (5)	0.0223 (5)	0.0192 (5)	−0.0002 (4)	−0.0009 (4)	−0.0011 (4)
C4	0.0226 (5)	0.0231 (5)	0.0201 (5)	−0.0001 (4)	0.0005 (4)	−0.0017 (4)
C5	0.0245 (5)	0.0251 (5)	0.0224 (5)	−0.0026 (4)	−0.0024 (4)	−0.0004 (4)
C4A	0.0236 (5)	0.0218 (5)	0.0199 (5)	−0.0032 (4)	−0.0023 (4)	−0.0002 (3)
C6	0.0279 (5)	0.0270 (5)	0.0232 (5)	−0.0045 (4)	−0.0076 (4)	0.0016 (4)
C7	0.0348 (5)	0.0279 (5)	0.0175 (5)	−0.0066 (4)	−0.0037 (4)	−0.0015 (4)
C8	0.0285 (5)	0.0260 (5)	0.0200 (5)	−0.0021 (4)	0.0004 (4)	−0.0029 (4)
C8A	0.0238 (5)	0.0221 (5)	0.0201 (5)	−0.0031 (4)	−0.0031 (4)	−0.0001 (4)
C31	0.0237 (5)	0.0242 (5)	0.0200 (5)	0.0021 (4)	−0.0006 (4)	−0.0009 (4)
C34	0.0204 (5)	0.0227 (5)	0.0208 (5)	0.0009 (3)	−0.0008 (4)	−0.0013 (3)
C341	0.0233 (5)	0.0212 (5)	0.0200 (5)	−0.0025 (4)	−0.0024 (4)	−0.0008 (4)

C342	0.0218 (5)	0.0270 (5)	0.0222 (5)	−0.0007 (4)	−0.0033 (4)	−0.0009 (4)
C343	0.0272 (5)	0.0315 (5)	0.0225 (5)	−0.0025 (4)	0.0022 (4)	−0.0036 (4)
C344	0.0360 (6)	0.0336 (5)	0.0178 (5)	−0.0057 (4)	−0.0040 (4)	−0.0014 (4)
C345	0.0288 (5)	0.0310 (5)	0.0247 (5)	−0.0011 (4)	−0.0089 (4)	0.0005 (4)
C346	0.0236 (5)	0.0262 (5)	0.0239 (5)	0.0013 (4)	−0.0028 (4)	−0.0015 (4)

Geometric parameters (Å, º)

O1—C8A	1.3749 (11)	C6—H6	0.9500
O1—C2	1.3765 (11)	C7—C8	1.3820 (14)
O2—C2	1.2103 (11)	C7—H7	0.9500
O31—C31	1.2237 (12)	C8—C8A	1.3867 (13)
N32—C31	1.3530 (13)	C8—H8	0.9500
N32—N33	1.3768 (11)	C34—C341	1.4649 (13)
N32—H1	0.857 (15)	C34—H34	0.9500
N33—C34	1.2753 (13)	C341—C346	1.3912 (13)
C2—C3	1.4629 (13)	C341—C342	1.4030 (13)
C3—C4	1.3492 (13)	C342—C343	1.3826 (13)
C3—C31	1.5003 (13)	C342—H342	0.9500
C4—C4A	1.4334 (13)	C343—C344	1.3908 (14)
C4—H4	0.9500	C343—H343	0.9500
C5—C6	1.3790 (13)	C344—C345	1.3890 (15)
C5—C4A	1.4036 (13)	C344—H344	0.9500
C5—H5	0.9500	C345—C346	1.3903 (13)
C4A—C8A	1.3978 (14)	C345—H345	0.9500
C6—C7	1.3960 (14)	C346—H346	0.9500

C8A—O1—C2	123.10 (7)	C8A—C8—H8	120.7
C31—N32—N33	118.22 (8)	O1—C8A—C8	117.65 (8)
C31—N32—H1	121.3 (9)	O1—C8A—C4A	120.69 (8)
N33—N32—H1	120.5 (9)	C8—C8A—C4A	121.66 (9)
C34—N33—N32	116.05 (8)	O31—C31—N32	123.05 (9)
O2—C2—O1	116.32 (8)	O31—C31—C3	120.11 (9)
O2—C2—C3	126.92 (8)	N32—C31—C3	116.83 (8)
O1—C2—C3	116.76 (8)	N33—C34—C341	119.21 (8)
C4—C3—C2	120.21 (9)	N33—C34—H34	120.4
C4—C3—C31	117.51 (8)	C341—C34—H34	120.4
C2—C3—C31	122.28 (8)	C346—C341—C342	119.23 (9)
C3—C4—C4A	121.77 (9)	C346—C341—C34	119.47 (8)
C3—C4—H4	119.1	C342—C341—C34	121.30 (9)
C4A—C4—H4	119.1	C343—C342—C341	119.88 (9)
C6—C5—C4A	119.97 (9)	C343—C342—H342	120.1
C6—C5—H5	120.0	C341—C342—H342	120.1
C4A—C5—H5	120.0	C342—C343—C344	120.75 (9)
C5—C4A—C8A	118.69 (9)	C342—C343—H343	119.6
C5—C4A—C4	123.84 (9)	C344—C343—H343	119.6
C8A—C4A—C4	117.47 (9)	C345—C344—C343	119.56 (9)
C5—C6—C7	120.12 (9)	C345—C344—H344	120.2

C5—C6—H6	119.9	C343—C344—H344	120.2
C7—C6—H6	119.9	C344—C345—C346	120.04 (9)
C8—C7—C6	121.01 (9)	C344—C345—H345	120.0
C8—C7—H7	119.5	C346—C345—H345	120.0
C6—C7—H7	119.5	C341—C346—C345	120.54 (9)
C7—C8—C8A	118.53 (9)	C341—C346—H346	119.7
C7—C8—H8	120.7	C345—C346—H346	119.7

C31—N32—N33—C34	177.57 (7)	C4—C4A—C8A—O1	−0.84 (14)
C8A—O1—C2—O2	179.69 (7)	C5—C4A—C8A—C8	−0.11 (14)
C8A—O1—C2—C3	−0.40 (13)	C4—C4A—C8A—C8	179.54 (8)
O2—C2—C3—C4	179.63 (9)	N33—N32—C31—O31	−1.83 (15)
O1—C2—C3—C4	−0.27 (13)	N33—N32—C31—C3	178.66 (7)
O2—C2—C3—C31	−0.41 (16)	C4—C3—C31—O31	−2.44 (14)
O1—C2—C3—C31	179.69 (7)	C2—C3—C31—O31	177.61 (9)
C2—C3—C4—C4A	0.36 (15)	C4—C3—C31—N32	177.08 (7)
C31—C3—C4—C4A	−179.59 (7)	C2—C3—C31—N32	−2.87 (14)
C6—C5—C4A—C8A	−0.67 (14)	N32—N33—C34—C341	178.28 (7)
C6—C5—C4A—C4	179.70 (8)	N33—C34—C341—C346	−179.53 (8)
C3—C4—C4A—C5	179.82 (8)	N33—C34—C341—C342	−0.13 (14)
C3—C4—C4A—C8A	0.18 (15)	C346—C341—C342—C343	0.63 (14)
C4A—C5—C6—C7	0.70 (14)	C34—C341—C342—C343	−178.78 (8)
C5—C6—C7—C8	0.06 (14)	C341—C342—C343—C344	0.20 (15)
C6—C7—C8—C8A	−0.82 (14)	C342—C343—C344—C345	−0.51 (15)
C2—O1—C8A—C8	−179.39 (7)	C343—C344—C345—C346	−0.01 (15)
C2—O1—C8A—C4A	0.97 (14)	C342—C341—C346—C345	−1.15 (14)
C7—C8—C8A—O1	−178.79 (7)	C34—C341—C346—C345	178.27 (8)
C7—C8—C8A—C4A	0.85 (15)	C344—C345—C346—C341	0.85 (15)
C5—C4A—C8A—O1	179.51 (8)		

Hydrogen-bond geometry (Å, º)

D—H···*A*	*D*—H	H···*A*	*D*···*A*	*D*—H···*A*
N32—H1···O2	0.857 (15)	2.062 (15)	2.7238 (10)	133.5 (12)
C34—H34···O2$^{\rm i}$	0.95	2.54	3.4417 (11)	159
C4—H4···O31	0.95	2.40	2.7415 (11)	101
C4—H4···O31$^{\rm ii}$	0.95	2.28	3.1377 (12)	149
C5—H5···O31$^{\rm ii}$	0.95	2.57	3.3456 (12)	139
C346—H346···O1$^{\rm i}$	0.95	2.63	3.5195 (11)	156

Symmetry codes: (i) −*x*, −*y*+1, −*z*+1; (ii) −*x*+2, −*y*, −*z*+1.